

Development of high-resolution gamma detector using sub-mm GAGG crystals coupled to TSV-MPPC array

To cite this article: A. Lipovec *et al* 2016 *JINST* **11** C03026

View the [article online](#) for updates and enhancements.

Related content

- [Performance of FBK high-density SiPM technology coupled to Ce:LYSO and Ce:GAGG for TOF-PET](#)
Alessandro Ferri, Alberto Gola, Nicola Serra *et al*.
- [Probing shallow electron traps in cerium-doped \$\text{Gd}_3\text{Al}_2\text{Ga}_3\text{O}_{12}\$ scintillators by UV-induced absorption spectroscopy](#)
Mamoru Kitaura, Kei Kamada, Shunsuke Kurosawa *et al*.
- [Luminescent properties of \$\text{Ce:Gd}_3\(\text{Al,Ga,Mg,M}\)_5\text{O}_{12}\$ crystal \(M = Zr, Hf\)](#)
Shunsuke Kurosawa, Kei Kamada, Yuui Yokota *et al*.

Recent citations

- [Experimental evaluation of \$\text{Gd}_3\text{Al}_2\text{Ga}_3\text{O}_{12}:\text{Ce}\$ \(GAGG:Ce\) single crystals coupled to a silicon photomultiplier \(SiPM\) under high gamma ray irradiation conditions](#)
A Metallinos *et al*



IOP | ebooks™

Bringing you innovative digital publishing with leading voices to create your essential collection of books in STEM research.

Start exploring the collection - download the first chapter of every title for free.

17TH INTERNATIONAL WORKSHOP ON RADIATION IMAGING DETECTORS
28 JUNE – 2 JULY 2015,
DESY, HAMBURG, GERMANY

Development of high-resolution gamma detector using sub-mm GAGG crystals coupled to TSV-MPPC array

A. Lipovec,¹ K. Shimazoe and H. Takahashi

*Department of Nuclear Engineering and Management, School of Engineering,
The University of Tokyo, 7-3-1 Hongo, Bunkyo-ku, Tokyo 113-8656, Japan*

E-mail: lipovec@sophie.q.t.u-tokyo.ac.jp

ABSTRACT: In this study a high-resolution gamma detector based on an array of sub-millimeter Ce:GAGG (Cerium doped $\text{Gd}_3\text{Al}_2\text{Ga}_3\text{O}_{12}$) crystals read out by an array of surface-mount type of TSV-MPPC was developed. MPPC sensor from Hamamatsu which has a 26 by 26 mm² detector area with 64 channels was used. One channel has a 3 by 3 mm² photosensitive area with 50 μm pitch micro cells. MPPC sensor provides 576 mm² sensing area and was used to decode 48 by 48 array with 0.4 by 0.4 by 20 mm³ Ce:GAGG crystals of 500 μm pitch. The base of the detector with the crystal module was mounted to a read out board which consists of charge division circuit, thus allowing for a read out of four channels to identify the position of the incident event on the board. The read out signals were amplified using charge sensitive amplifiers. The four amplified signals were digitized and analyzed to produce a position sensitive event. For the performance analysis a ¹³⁷Cs source was used. The produced events were used for flood histogram and energy analysis. The effects of the glass thickness between the Ce:GAGG and MPPC were analyzed using the experimental flood diagrams and Geant4 simulations. The glass between the scintillator and the detector allows the spread of the light over different channels and is necessary if the channel's sensitive area is bigger than the scintillator's area. The initial results demonstrate that this detector module is promising and could be used for applications requiring compact and high-resolution detectors. Experimental results show that the detectors precision increases using glass guide thickness of 1.35 mm and 1.85 mm; however the precision using 2.5 mm are practically the same as if using 0.8 mm or 1.0 mm glass guide thicknesses. In addition, simulations using Geant4 indicate that the light becomes scarcer if thicker glass is used, thus reducing the ability to indicate which crystal was targeted. When 2.5 mm glass thickness is used, the scarce light effect becomes dominant for the precision of the detector.

KEYWORDS: Image reconstruction in medical imaging; Performance of High Energy Physics Detectors; Simulation methods and programs; Gamma camera, SPECT, PET PET/CT, coronary CT angiography (CTA)

¹Corresponding author.

Contents

1	Introduction	1
2	Materials and methods	1
2.1	GAGG crystals	1
2.2	MPPC array	2
3	The construction of the detector	2
3.1	Experimental setup	3
3.2	Simulation setup using GEANT4	3
4	Results	4
4.1	Analysis of the device performance	4
5	Analysis of the simulated light distribution	5
6	Conclusions	8

1 Introduction

A photodetector is often used in conjunction with scintillators to convert light emitted by the scintillator upon interaction with radiation to electrical signals. Silicon photomultipliers (SiPMs) are relatively new silicon based semiconductor photodetectors which are of great interest for high energy physics, astrophysics and medical applications because of their properties such as high gain and quantum efficiency (but low fill factor), fast response, compactness and insensitivity to magnetic fields. Multi-pixel photon counter (MPPC) is a promising SiPM and is extensively used in the biomedical fluorescence detection, fluorescence lifetime measurements, confocal microscopes, positron emission tomography (PET), single photon emission CT (SPECT) and high energy physics [1–9].

The aim of this study is to develop a high-resolution gamma detector based on an array of sub-millimeter Ce:GAGG (Cerium doped $\text{Gd}_3\text{Al}_2\text{Ga}_3\text{O}_{12}$) crystals read out by an array of surface-mount type of MPPC. To achieve this aim, the device performance based on the glass thickness between the components was analyzed using experiments. In addition, Geant4 simulations were used to analyze the effects of the glass in such system.

2 Materials and methods

2.1 GAGG crystals

An ideal scintillator should have high luminosity, high density and high effective atomic number, fast rise and decay time constants, a peak emission wavelength that matches with the spectral

Table 1. Properties of the Ce:GAGG crystal.

Scintillator	Ce:GAGG
Density (g/cm ³)	6.63 [5]
Light yield (photons/MeV)	46 000 [5]
Decay time constant (ns)	88 (91%) and 258 (9%) [7]
Emission peak (nm)	520–530 [8]
Intrinsic energy resolution (%@662keV)	4.9 [9]

sensitivity of the photo detector and low non-proportionality. In addition, the scintillation material should be inexpensive to manufacture, non-hygroscopic, rugged and preferably produce no intrinsic radiation [5]. The Ce:GAGG scintillator has several advantages compared to other scintillators. It has a large light output and longer emission light wavelength [6]. When it is used with a typical SiPM, the longer scintillation light wavelength produces a larger signal. Typical values of Ce:GAGG scintillator are given in the table 1. It can be seen that Ce:GAGG scintillator has a high density, high light yield, and short decay time.

For this study an array of 48 by 48 Ce:GAGG scintillator crystals was designed and fabricated (figure 1). The dimensions of one crystal are 0.4 by 0.4 by 20 mm³ which is wrapped in a 50 μ m layer of barium sulfate (BaSO₄) reflector. The pitch of the scintillator array is 500 μ m.

2.2 MPPC array

The MPPC sensor is a photon-counting device which uses multiple avalanche photodiode pixels (APD) operating in Geiger mode each with an integrated quench circuit and connected together in parallel on a single piece of silicon. MPPC is compact, insensitive to gamma rays and can detect extremely weak light. In addition, the signals produced with the MPPC are proportional to the number of the incident photons which is important for applications requiring a photon counting capability.

For this study a TSV-MPPC sensor from Hamamatsu *S12642-0808PA-50 [10] was used (figure 2). This sensor has a 26 by 26 mm² detector area with 64 channels, where one channel has a 3 by 3 mm² photosensitive area. The micro cell pitch is 50 μ m which gives 3600 micro cells per channel. Overall, MPPC sensor provides a 576 mm² sensing area and was used to decode 48 by 48 array with 0.4 by 0.4 by 20 mm³ Ce:GAGG crystals of 500 μ m pitch.

3 The construction of the detector

In order to allow the 64-channels MPPC detector to identify the 2304 Ce:GAGG crystals, a glass was placed between them and coupled with silicone glue (Toshiba Silicone Oken6262, Japan). The glass allows the spread of the light from the crystals over several different channels (figure 3). The base of the detector with the crystal module was mounted onto a read out board which consists of a charge division circuit with four channel read out [11]. Such approach allowed the signals of the 64-channels to be combined in such a way that the position of the active crystal could be identified. In addition, the reconstructed positions are relative positions; therefore a flood diagram is used to

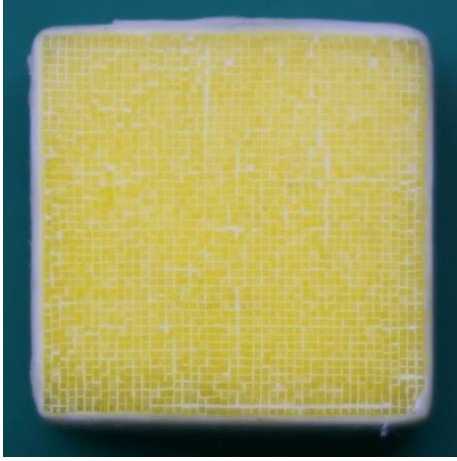


Figure 1. 48 by 48 array with 0.4 by 0.4 by 20 mm³ Ce:GAGG crystals of 500 μ m pitch.

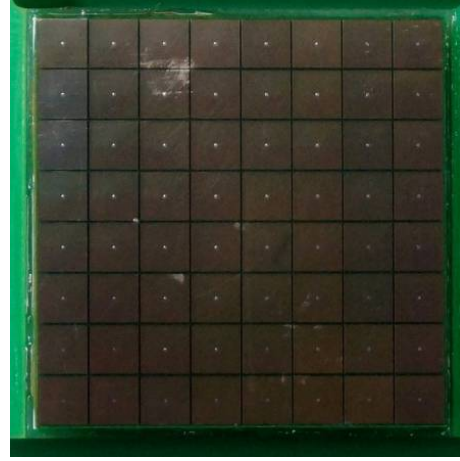


Figure 2. 64-channels MPPC detector with 26 by 26 mm² sensor size.

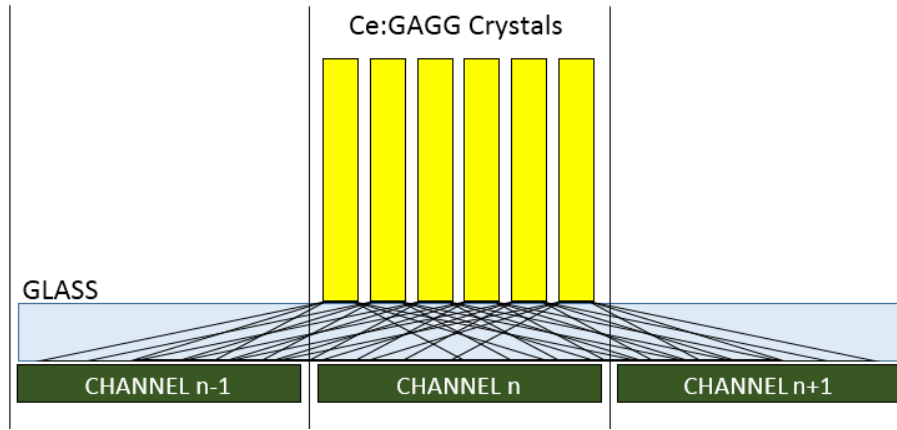


Figure 3. The spread of light from the crystals through the glass over several different channels.

reconstruct the real position on the detector. The resolution of the detector can be also tested using the flood diagram.

3.1 Experimental setup

The four read out signals from the detector were amplified using charge sensitive amplifiers (Ortec Model 570 amplifier, Ametek, PA, U.S.A.) and digitized using an oscilloscope (HDO 4054, Teledyne LeCroy, CA, U.S.A.). The signals were analyzed to produce a position sensitive event. For the performance analysis a ¹³⁷Cs source was used, and the operating voltage was set to 66.5 V. In each experiment 5 million events were collected while setup was at room temperature. The produced events were used for flood histogram and energy analysis.

3.2 Simulation setup using GEANT4

In this study, simulations using GEANT4 framework were used to investigate and to analyze light production and propagation in the Ce:GAGG crystals and its spreading through the glass. The dimension of one Ce:GAGG crystal was 0.4 by 0.4 by 20 mm³. The crystal was wrapped using a

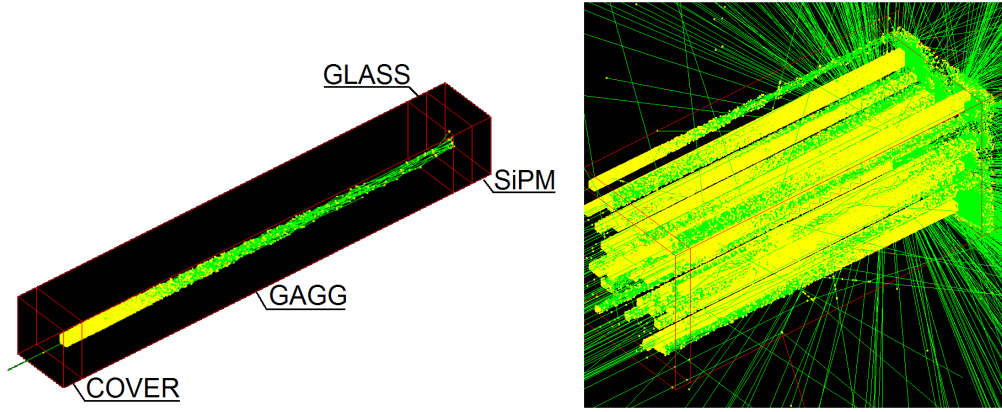


Figure 4. Simulation of light production and propagation using GEANT4 framework.

50 μm layer of barium sulfate (BaSO_4) which makes the pitch of the crystals to be 500 μm . Several of these Ce:GAGG crystals were set together to form the 18 by 18 light converting crystal of 9 by 9 mm^2 area. The reduced crystal array size was chosen as the same effects would be present while the need for the time and resources would be lowered. One end was covered with a layer of barium sulfate while the other was left open. Between the opened end and the surface of the detector a glass was placed. The thickness of the glass varied and was between 0 mm and 2.5 mm. The areas of the glass and the detector were the same as the crystal array (81 mm^2) which was equivalent to the 3 by 3 SiPMs (sized 9 by 9 mm^2). The parameters used to simulate the scintillation in the Ce:GAGG are shown in the table 1. In addition, glass refractive index, Ce:GAGG refractive index and GAGG reflection probability were set to 1.54, 1.87 and 0.8, respectively.

In the simulation (see figure 4), the initial light was produced using gamma rays (662 keV) and was directed perpendicular to the front surface of the Ce:GAGG array. The light production was random with uniform distribution over that surface. A gamma ray interacted with Ce:GAGG crystal and sometimes generated an electron. The free electron inside the Ce:GAGG crystal generated light by losing its kinetic energy. The light traveled through the crystal until it reached one end. The light entered the glass, refracted and spread over the detector surface. The different light spreads over the detector was analyzed by changing the thickness of the glass.

4 Results

4.1 Analysis of the device performance

Figure 5 shows the experimental results using different thickness of glass: (a) flood diagrams of 48 by 48 array with 0.4 by 0.4 by 20 mm^3 Ce:GAGG crystals; (b) zoomed flood diagrams of 2 by 2 Ce:GAGG crystals; (c) energy spectrums of the zoomed 2 by 2 Ce:GAGG crystals. Five different glass thicknesses were tested: 0.8, 1.0, 1.35, 1.85 and 2.5 mm. The experimental results show quite similar flood diagrams in all the analyzed glass thickness (figure 5a). Only the zoomed flood diagrams show more difference (figure 5b). In these diagrams (figures 5a and 5b), the relative coordinates of the flood diagrams were discretized over 900 pixels. The differences between the flood diagrams were evaluated using peak to valley ratios (PVRs). PVR value indicates how well

Table 2. Peak to valley ratios (PVRs) of experimental and simulated flood diagrams.

	Glass thickness, mm				
	0.80	1.00	1.35	1.85	2.50
PVR (experimental)	1.5 ± 0.1	1.5 ± 0.1	1.6 ± 0.1	1.7 ± 0.1	1.5 ± 0.1
Ideal PVR (simulated)	16.0 ± 2.0	11.0 ± 2.0	8.0 ± 2.0	4.1 ± 0.5	2.6 ± 0.4

two crystals can be separated and was calculated for a few dozen randomly chosen crystals for each glass thickness. The average PVR values and their standard deviations are presented in the table 2. PVRs are low and similar (~ 1.5) in all analyzed glass thicknesses with significant statistical increase from 1.35 mm to 1.85 mm. Finally, the spectrums of the zoomed pixels (figure 5c) have similar properties in all the analyzed flood diagrams: the initial peak is the noise, the peak at ~ 3 V is the backscatter peak, the drop at ~ 5 V represents the Compton edge, and the peak at ~ 7 V is the ^{137}Cs peak.

To conclude, sufficiently high PVRs values and characteristic spectrums indicate that the device is working properly. Similar channel and crystal sizes were analyzed in [9] study; there 1.5 mm glass thickness was used to achieve PVR of 3.8. However, in this study to make a more compact setup 4 times larger detector was used with Anger readout principle. This allows to reduce readout schematics, however, as experiments indicate, this also reduces PVR values. To analyze other effects limiting the detector's resolution Geant4 simulations were performed.

5 Analysis of the simulated light distribution

The power of Anger principle is roughly determined by the ratio of the crystal size to the channel size [9]. However, the light spreading effects are not clear.

Effects of the glass thickness on the light spreading over the detector can be analyzed by targeting one Ce:GAGG crystal. Several different glass thicknesses were tested by irradiating the one crystal (area of 0.5 by 0.5 mm which also included the wrapping of barium sulfate) with 10,000 gamma rays of 662 keV. Only around 48% of the initial gamma rays produced secondary light, that is the crystal event efficiency from incident gamma rays is around 0.48 (table 3). This effectiveness was observed in all the simulations. The distribution of light intensity was measured over the center line by averaging the positions of all the produced light. The results are shown in the figure 6. By using a thicker glass the distribution of light widens, that is the intensity of light had been reduced at the center of the crystal and increased further from it. However, the light is highly focused which can be seen from the full width at half maximum (FWHM) of the light distribution (table 3). The higher spread allows for the detector to reconstruct the event more precisely, but the light becomes more scattered reducing the precision. One gamma event will produce multiple light events at different positions on the detector. The average position of these events will represent the initial gamma event. However, the signal generation in the microcells and its final form, which the charge division circuit generates, were not simulated using Geant4; therefore only ideal event reconstruction can be performed using the simulation data. The standard deviation of this ideally reconstructed event shows how accurately it is possible to reconstruct the initial position (table 3). The increase of the standard deviation by increasing the glass thickness indicates that this reconstruction ability

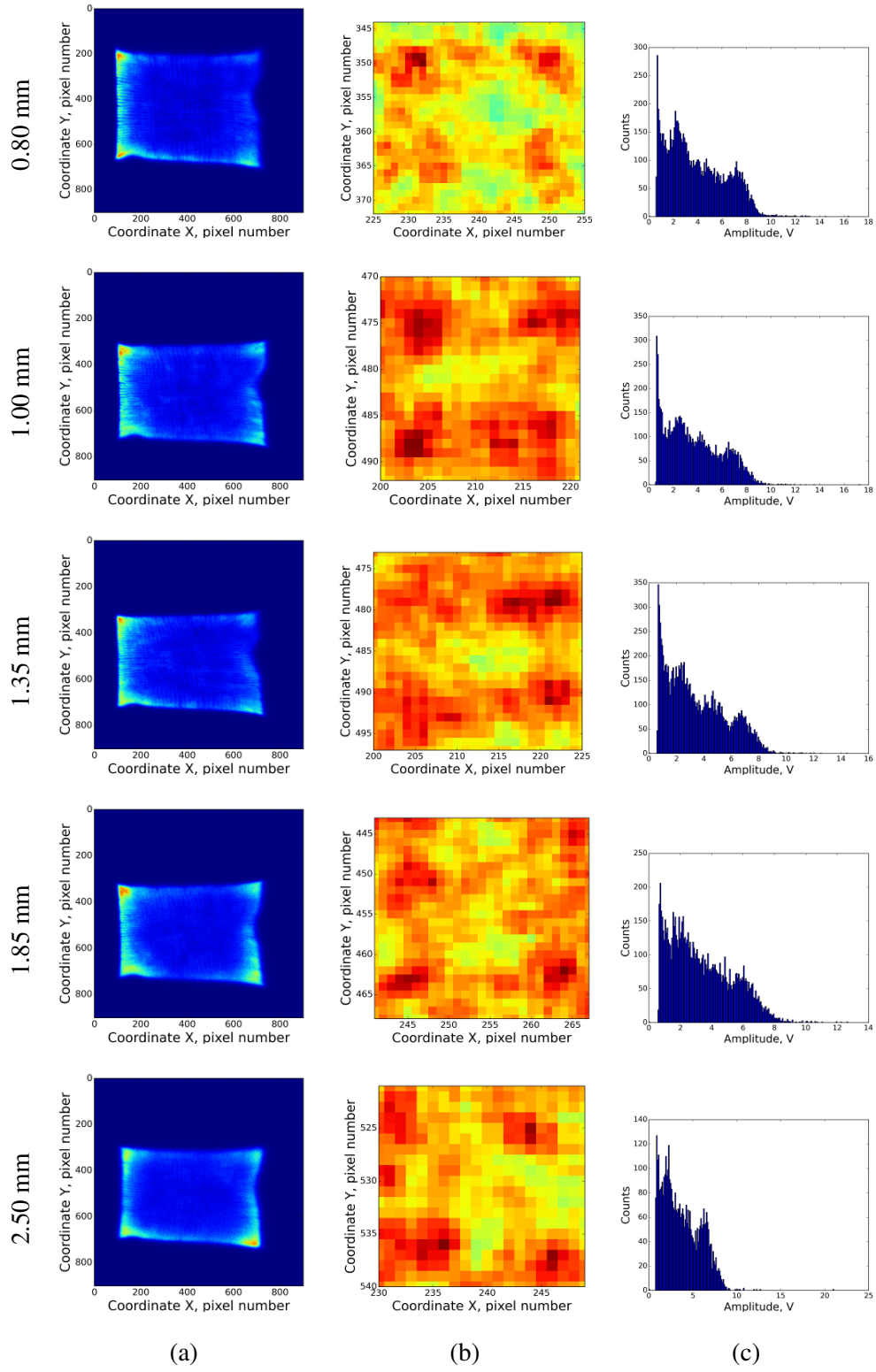


Figure 5. (a) flood diagrams of 48 by 48 array with 0.4 by 0.4 by 20 mm³ Ce:GAGG crystals; (b) zoomed flood diagrams of 2 by 2 Ce:GAGG crystals; (c) energy spectra of the zoomed 2 by 2 Ce:GAGG crystals. The relative coordinates of the flood diagrams are discretized over 900 pixels.

Table 3. Calculated event efficiency from incident photon, standard deviation of the ideally reconstructed events and the FWHM of the distribution of light intensity from the simulation results of one 0.4 by 0.4 by 20 mm³ Ce:GAGG crystal using different glass thickness.

	Glass thickness, mm					
	0.00	0.80	1.00	1.35	1.85	2.50
Event efficiency from incident gamma rays	0.46	0.49	0.47	0.48	0.48	0.48
Distribution of light intensity FWHM, mm	0.40	0.61	0.65	0.74	0.87	1.10
Standard deviation of the ideally reconstructed events, mm	0.11	0.15	0.16	0.21	0.22	0.25

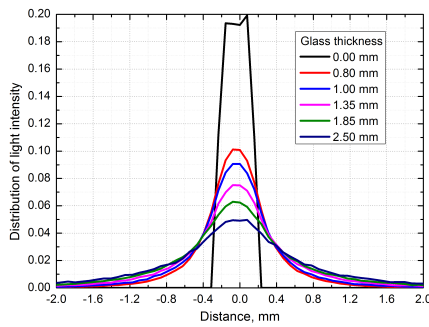


Figure 6. Effect of the glass thickness on the distribution of light intensity using one crystal (sized 0.4 by 0.4 mm).

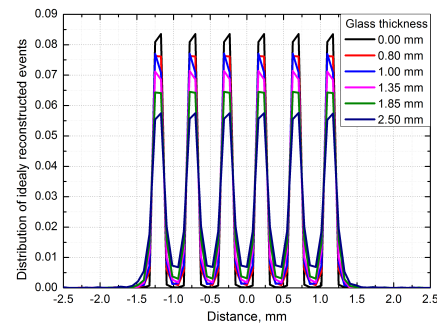


Figure 7. Effect of the glass thickness on the ideally reconstructed events of 6 closely placed crystals (sized 0.4 by 0.4 mm with 0.5 mm pitch).

decreases by increasing the glass thickness. When such crystals are placed closely, with thicker glass the reconstructed events overlap more (see figure 7). That is, the simulated results show that the ability to separate the closely packed crystals is reduced by the additional glass. Therefore, the increased ability of the detector to reconstruct the crystal in Anger principle by increasing the glass thickness is reduced by the scarcity of the light.

To analyze a more realistic system, 18 by 18 Ce:GAGG crystals array was targeted with 500,000 gamma rays which produced light on the surface of the detector. By using the ideal event reconstruction (by averaging the light from one event) the ideal flood diagrams were evaluated (figure 8). In these diagrams crystal can be separated clearly. The statistical analysis of the PVRs of the ideal flood diagrams are shown in the table 2. These PVRs are much higher than the experimental values and decrease with the increase of the glass thickness. The experimental and simulated flood diagrams should not be compared side by side as experimental results are of relative positions due to charge division read out system which was not evaluated in this study.

To sum up simulation results, the increase of the glass thickness reduces the ability to reconstruct the incident gamma event. The light produced by the gamma event in the crystal is limited and when the glass thickness increases the bigger spread of the light becomes too scarce to reconstruct the event precisely. The simulated ideal PVR values refer to the limit which ideal detectors could achieve due to physical light spreading before the detection.

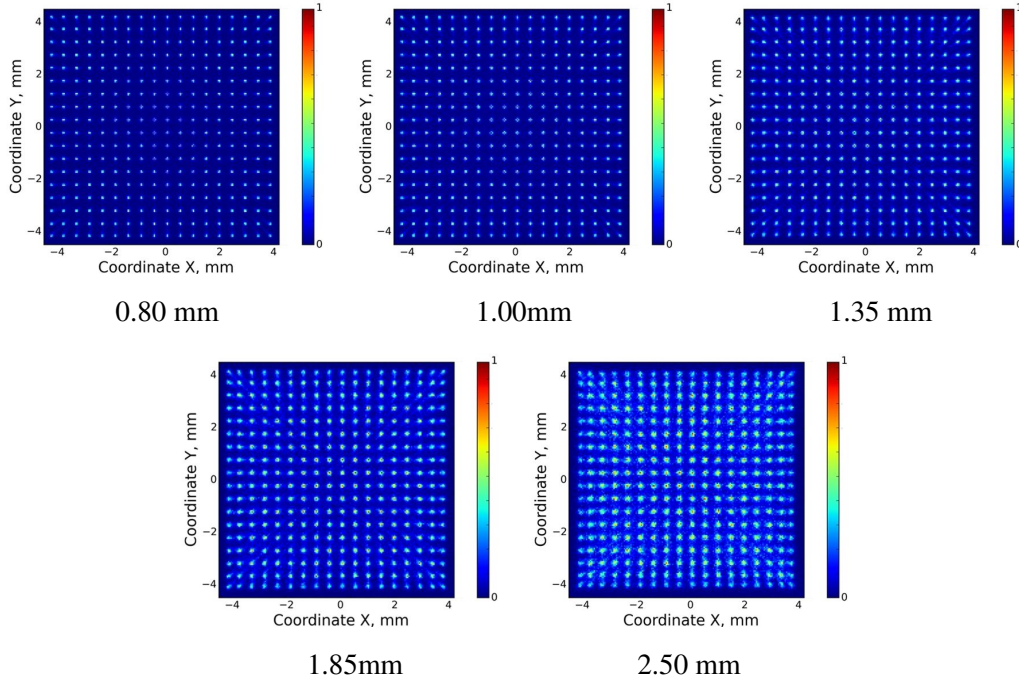


Figure 8. Ideal reconstruction of the Ce:GAGG crystals (using averaging of the simulated light events).

6 Conclusions

The initial results demonstrate that the newly developed detector module is promising for sub-mm resolution gamma ray imaging and could be used for compact and high-resolution applications. The crystals can be separated in the flood diagrams which indicate a possibility of 0.5 mm precision. The effects of the glass thickness are quite small. The PVRs are quite low in all the analyzed glass thickness. A significant increase in the resolution can be observed in the 1.35 mm and 1.85 mm glass thicknesses. Therefore, a glass thickness between 1.35 mm and 1.85 mm is recommended to be used for the best resolution. Simulation results show that the increase of the glass thickness increase the spread of the light over the surface of the detector but makes the light more scarce which reduces the ability to indicate the light producing crystal. In order to make a more compact high resolution detector a large number of sensitive channels via readout channels and a large number of crystals per channel were used. However, as experimental and simulated results indicate, the detector resolution is limited by the Anger principle readout of the large number of channels and the scarcity of the light.

References

- [1] K. Kamada et al., *Development of a prototype detector using APD-arrays coupled with pixelized Ce:GAGG scintillator for high resolution radiation imaging*, *IEEE Trans. Nucl. Sci.* **61** (2014) 348.
- [2] C. Bosio et al., *First results of systematic studies done with silicon photomultipliers*, *Nucl. Instrum. Meth. A* **596** (2008) 134.
- [3] T.Y. Song et al., *Sub-millimeter resolution PET detector module using multi-pixel photon counter array*, *IEEE Nucl. Sci. Symp. (NSS/MIC)* (2008) 4933.

- [4] J. Kataoka et al., *Recent progress of MPPC-based scintillation detectors in high precision X-ray and gamma-ray imaging*, *Nucl. Instrum. Meth. A* **784** (2014) 248.
- [5] J.Y. Yeom et al., *First performance results of Ce:GAGG scintillation crystals with silicon photomultipliers*, *IEEE Trans. Nucl. Sci.* **60** (2013) 988.
- [6] S. Yamamoto et al., *Development of an ultrahigh resolution block detector on 0.4 mm pixel Ce:GAGG scintillators and a silicon photomultiplier array*, *IEEE Trans. Nucl. Sci.* **60** (2013) 4582.
- [7] T. Kato et al., *High position resolution gamma-ray imagers consisting of a monolithic MPPC array with submillimeter, pixelized scintillator crystals*, *IEEE Nucl. Sci. Symp. (NSS/MIC)* (2012) 3146.
- [8] B. Seitz et al., *Performance evaluation of novel SiPM for medical imaging applications*, *IEEE Nucl. Sci. Symp. (NSS/MIC)* (2013) 1.
- [9] S. Yamamoto et al., *Development of an ultrahigh-resolution Si-PM-based dual-head GAGG coincidence imaging system*, *Nucl. Instrum. Meth. A* **703** (2013) 183.
- [10] Hamamatsu Photonics K.K., *MPPC and MPPC module for precision measurement*, <http://www.hamamatsu.com/jp/en/product/category/3100/4004/index.html>.
- [11] S. Siegel et al., *Simple charge division readouts for imaging scintillator arrays using a multi-channel PMT*, *IEEE Trans. Nucl. Sci.* **43** (1996) 1634.